

Imprinting magnetic information in manganites with X-rays

M. Garganourakis, V. Scagnoli, S. W. Huang, and U. Staub*
Swiss Light Source, Paul Scherrer Institut, CH 5232 Villigen PSI, Switzerland

H. Wadati
*Department of Applied Physics and Quantum-Phase Electronics Center (QPEC),
University of Tokyo, Hongo, Tokyo 113-8656, Japan*

M. Nakamura
*Cross-Correlated Materials Research Group (CMRG),
Advanced Science Institute, RIKEN, Wako 351-0198, Japan*

V. A. Guzenko
Laboratory for Micro- and Nanotechnology, Paul Scherrer Institut, 5232 Villigen PSI, Switzerland

M. Kawasaki and Y. Tokura
*Department of Applied Physics and Quantum-Phase Electronics Center (QPEC),
University of Tokyo, Hongo, Tokyo 113-8656, Japan and
Cross-Correlated Materials Research Group (CMRG),
Advanced Science Institute, RIKEN, Wako 351-0198, Japan
(Dated: June 20, 2018)*

The effect of x-rays on an orbital and charge ordered epitaxial film of a $\text{Pr}_{0.5}\text{Ca}_{0.5}\text{MnO}_3$ is presented. As the film is exposed to x-rays, the antiferromagnetic response increases and concomitantly the conductivity of the film improve. These results are discussed in terms of a persistent x-ray induced doping, leading to a modification of the magnetic structure. This effect allows writing electronic and magnetic domains in the film and represents a novel way of manipulating magnetism.

Many interesting electronic and magnetic phenomena occur in transition metal oxides, such as colossal magnetoresistance, superconductivity and metal-insulator transitions. These phenomena result from the intimate interplay between charge, orbital, and magnetic degrees of freedom, and their coupling to structural distortions. Such complex interactions lead to rich phase diagrams and the tuning of electronic properties close to phase boundaries [1].

In manganites, the entangled charge, orbital and magnetic degrees of freedom lead to a variety of phases and instabilities at its boundaries. Temperature, electric and magnetic fields, and electromagnetic radiation can change the electronic properties. In particular it has been shown that electromagnetic radiation can be used to manipulate the electronic and structural properties of perovskite type manganites. On the ultra fast time scale, terahertz pulses can directly excite vibrational excitations leading to a metal-insulator transition [2] where structural phase transitions can be induced by optical pulses [3]. In certain compositions these transitions can be persistent [4]. However in most cases, changes occur as a direct consequence of the pulse and responses are not permanent. A permanent phase change can be induced by x-rays. It has been shown that hard x-ray exposure can destroy the crystallographic superstructure of the charge and orbital ordered phase at low temperatures for $\text{Pr}_{1-x}\text{Ca}_x\text{MnO}_3$ for x close to the ferromagnetic

insulating phase boundary [5]. Similar effects were also observed via electron radiation [6]. More generally, it is well known that x-ray diffraction can easily break bonds and destroy crystal structure, a significant drawback e.g. in protein crystallography [7].

$\text{Pr}_{1-x}\text{Ca}_x\text{MnO}_3$, $0.3 \leq x \leq 0.5$, is a bandwidth controlled insulator with a CE-type charge and orbital order, forming zig-zag chains in the planes [8]. For $x=0.5$ the magnetic moments are antiferromagnetically ordered and lie fully in the ab-plane, Fig.1(a). By lowering the doping level x , the moments rotate out of the plane and, around $x=0.3$, the system transforms into a ferromagnetic insulator [9]. To manipulate the magnetic state of the $\text{Pr}_{0.5}\text{Ca}_{0.5}\text{MnO}_3$ thin film and measure its response, we use Resonant X-ray Diffraction (RXD) at the Mn edge $2p_{3/2}$ - $3d$ L_3 transition. RXD is a very sensitive tool to study the magnetic and orbital order and has been already used extensively to study this thin film [10] and other doped PrMnO_3 perovskites [11] - [13].

An epitaxial thin film of $\text{Pr}_{0.5}\text{Ca}_{0.5}\text{MnO}_3$ was deposited onto an $(\text{LaAlO}_3)_{0.3}$ - $(\text{SrAl}_{0.5}\text{Ta}_{0.5}\text{O}_3)_{0.7}$ substrate with (0 1 1) direction normal to the surface by Pulsed Laser Deposition (PLD). These experiments were performed at the Swiss Light Source, Paul Scherrer Institut, using the RESOXS-endstation [14] at the SIM beamline [15]. Gold contacts spaced $700 \mu\text{m}$ apart were deposited on the $\text{Pr}_{0.5}\text{Ca}_{0.5}\text{MnO}_3$ film's surface with a $100 \mu\text{m}$ gap between the electrodes to record the electrical

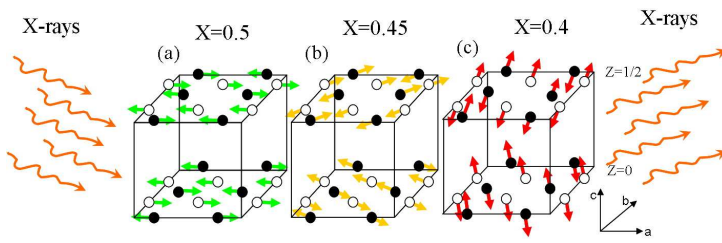


FIG. 1. Pictorial view of the x-ray induced electron doping with canting of the manganese magnetic moments of $\text{Pr}_{1-x}\text{Ca}_x\text{MnO}_3$, $0.4 \leq x \leq 0.5$, and corresponding changes in the magnetic structure.

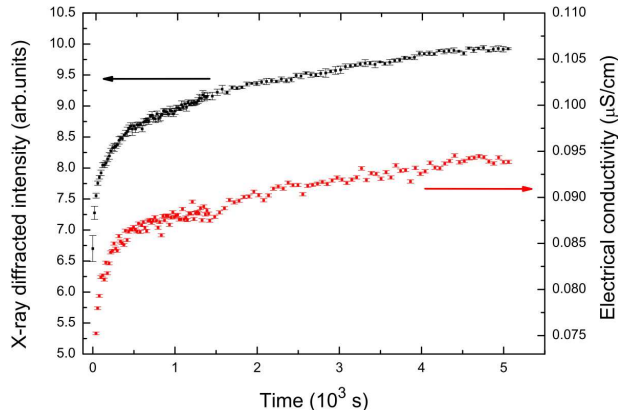


FIG. 2. X-ray exposure dependence of the $(1/4 \ 1/4 \ 0)$ reflection (left hand-side axis, black curve) and in-situ collected electrical conductivity (right hand-side axis, red curve) of epitaxial $\text{Pr}_{0.5}\text{Ca}_{0.5}\text{MnO}_3$ thin film at $T=50$ K. The energy of the X-ray beam was tuned to the resonance of Mn L_3 edge (642.5 eV) with incoming π polarization.

conductivity. An x-ray beam of size $100 \times 50 \ \mu\text{m}$ ($\sim 6 \times 10^{12}$ photons/s) was centered into the gap, to simultaneously expose and collect the diffracted Bragg intensities. The in-situ electrical conductivity between the electrodes was collected without x-rays impinging on the sample). More details about the measurement protocol are given in the supplementary information.

In Fig.2 we present the dependence of the orbital and magnetic $(1/4 \ 1/4 \ 0)$ Bragg peak intensity and the conductivity on x-ray exposure. The polarization of the incident beam was set in the scattering plane, so called π -geometry, with an incident x-ray energy of 642.5 eV (consult Supplementary Figure 1 for further detail).

Two remarkable phenomena are observed as a function of x-ray exposure: first an increase in the conductivity and second, an enhancement of the magnetic/orbital Bragg peak intensity. The increase in conductivity might be expected since past studies showed this effect on $\text{Pr}_{1-x}\text{Ca}_x\text{MnO}_3$ for $x=0.3$, close to the phase boundary to the ferromagnetic and insulating phase [5]. Surprisingly, the magnetic/orbital $(1/4 \ 1/4 \ 0)$ peak intensity enhances as a function of x-ray exposure time, in con-

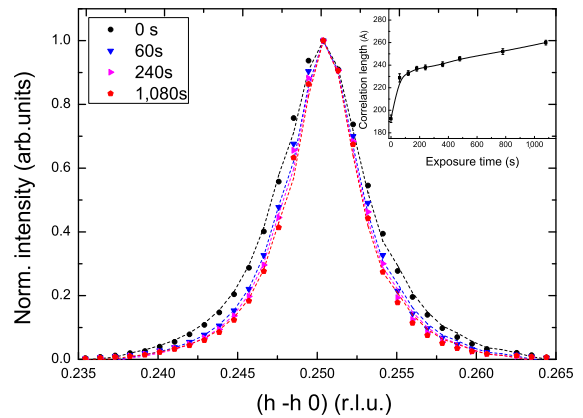


FIG. 3. Reciprocal space $(h \ -h \ 0)$ scan of the $(1/4 \ 1/4 \ 0)$ reflection for different exposure times and x-ray energy 642.5 eV using incident π polarization, taken at $T=50$ K. The maximum intensity is normalized to unity. The inset presents the evolution of the correlation length with respect to x-ray exposure time.

trast to the suppression of the structural superlattice reflection observed in $\text{Pr}_{0.7}\text{Ca}_{0.3}\text{MnO}_3$ [5]. In addition, the width of the Bragg peak decreases with increasing x-ray exposure as shown in Fig.3, whilst the integrated intensity still increases (see Supplementary Figure 2). This directly relates to an increase in the correlation length of the antiferromagnetic/orbital order (Fig.3 inset). In other words, the x-ray illumination improves the antiferromagnetic and/or orbital order of the system despite its expected destructive effect on the crystalline structure.

What is the microscopic origin of this unexpected result? The $(1/4 \ 1/4 \ 0)$ reflection has a magnetic and an orbital contribution [11, 12]. The orbital scattering of these reflections is well understood and a signal occurs only in the rotated $(\pi\sigma')$ and $(\pi'\sigma)$ polarization channels, each with equal an intensity [16]. Therefore, the magnetic scattering is on average larger in the π incident channel since at resonance the $\sigma\sigma'$ channel is forbidden. As the signal probed with π polarization is increasing much stronger than the one probed by σ , we can associate the changes to be mainly of magnetic origin (see Supplementary Figure 5). This view is supported by the increase in conductivity which actually indicates a reduction of orbital order and its contribution to this reflection. This excludes the possibility of x-ray annealing since that would improve the orbital order making the material more insulating.

For the resonant magnetic scattering, dominated by electric dipole transitions (E1), the magnetic scattering amplitude can be written as [17],

$$F_{\epsilon\epsilon'} \propto -i(\epsilon' \times \epsilon) \cdot \mathbf{F}_m \quad (1)$$

where ϵ' and ϵ are unit vectors of the incident and

scattered polarization of the x-rays, respectively and \mathbf{F}_m is the magnetic structure factor.

To obtain quantitative information we should calculate the magnetic structure factor

$$\mathbf{F}_m = \sum_j \mathbf{m}_j e^{i\mathbf{r}_j \cdot \mathbf{q}} \quad (2)$$

where \mathbf{m}_j is a tensor representing the magnetic moment at site j identified by \mathbf{r}_j and \mathbf{q} is the wavevector. Considering the structural phase factors and direction of the moment, e.g. \mathbf{F}_m , all contributions of the (1/4 1/4 0) reflection for the magnetic structure of $\text{Pr}_{1-x}\text{Ca}_x\text{MnO}_3$ for $x=0.5$, Fig.1(a), annihilate ($\mathbf{F}_m=0$). For the canted structure of the lower doping levels (such as in Fig.1(b),(c)), the structure factor contains a single component which is proportional to the magnetic moment components along the c-axis, $\mathbf{F}_m=(0,0,F_m)$, and only the Mn^{3+} ions contribute to the magnetic signal. This indicates that the enhancement of the magnetic peak intensity arises from the ferromagnetically coupled c-axis components of the Mn^{3+} spins in the CE-type antiferromagnet. The calculated value of the ratio between π and σ incident polarization Bragg intensities is consistent to the observed ratio for $T \leq T_N$ (Supplementary Figure 3) for this model consideration.

The basic mechanisms for the observed increase of the magnetic moment components along the c-axis has to be discussed in relation to the observed increase in the conductivity. The increase in conductivity is expected to be directly related to the creation of defects in the charge and orbital order. The effect of indirect electric fields on the sample due to charge can be excluded as the application of 10 KV/cm does not lead to an increase in scattering intensity. Such a scenario is consistent with the previously observed effect on the destruction of the corresponding crystallographic superstructure of the $x=0.3$ compound [5]. The creation of these defects excite deep donor levels which act as impurities in the material. This mechanism is quite similar to the behaviour of the *DX* centres in III-V semiconductors [18]. The x-ray-induced deep donor level impurities will be ionized and the corresponding electrons excited to the conduction band, resulting in the X-rays *photodoping* the material. This doping mimics a decrease in Ca concentration. The strong coupling of the electrons to the manganite lattice leads to a *metastable* state, which includes a local deformation of the lattice due to the ‘‘orbital/charge’’ defect, consistent with the fact that when the beam is turned off no recovery occurs. This doping effect can also naturally explain the enhancement of the magnetic intensity. Decreasing the Ca concentration, as well as our photodoping, leads to an increase in the spin canting in $\text{Pr}_{1-x}\text{Ca}_x\text{MnO}_3$, as visualized in Fig.1. For these materials, it is well known that increasing electron doping leads to a more metallic state

since it favours the double exchange interaction allowing electrons with neighboring parallel spins to hop. In contrast, electrons with antiferromagnetic spin alignments are frozen by the competing superexchange interaction. The increase of the (1/4 1/4 0) magnetic reflection reflects the alignment of the ferromagnetic spin component at least along the c-axis. The increase of the magnetic correlation length for increasing X-ray exposure is more difficult to understand. It may indicate that the phase transition, between the $x=0.5$ doping level and the in-plane antiferromagnetic order to the spin canted structure, is first order. Increasing the electron doping level would make then the material being in a single magnetic state with larger domain sizes, whereas for $x=0.5$ both domains may co-exist, leading to smaller ‘‘nano’’ domains.

In Fig.4 we present the contour plots of the collected X-ray intensity of the (1/4 1/4 0) reflection by rastering the sample through the beam. For this measurement we used lower x-ray photon flux (3×10^{12} photons/s) to reduce the effect of X-rays on the sample. The low intensity regions seen in Fig.4 are locations where the sample is expected to be shadowed by the gold contacts and the indium wires. In order to write magnetic information, we have exposed two different portions of the sample to the x-ray beam (indicated by the arrows in Fig.4). A clear increase of the scattered intensity is observed solely at the position of the x-ray exposure. After successfully writing magnetic information and its in-situ observation we tested the possibility to erase the written information. For this purpose we heated the sample above the orbital order (OO) transition temperature $T_{OO} \simeq 210$ K and rastered the sample again after cooling back to $T=50$ K, Fig.4(c). An intensity distribution identical to that before the x-ray exposure was observed, Fig.4(a), indicating a full recovery of the sample to the virgin state. This is also consistent with the view that the x-ray induced defects are local charge and orbital defects in the electronic ordering pattern.

Finally, Figure 5(a) displays a mesh scan of the virgin state of the film, whereas Fig.5(b) shows the same region now exposed to four different spatially segregated x-ray flux conditions. The difference between positions (i) and (ii) represents a change of x-ray flux density by a factor of two, whereas the differences between (ii), (iii) and (iv), represent a change of exit slit of the beamline, leading to an increase in vertical spot size. The time dependence of the low flux density exposure for position (i) is very different from the others showing clear saturation behavior after 100 s, Fig.5(c). This indicates that the process of interaction between the observed canting of the magnetic moments by x-rays is a strongly non-linear process.

To summarize, in this letter we describe a novel way to imprint magnetic and electronic information in strongly correlated manganites. The x-ray illumination photodopes an epitaxial thin film of $\text{Pr}_{0.5}\text{Ca}_{0.5}\text{MnO}_3$

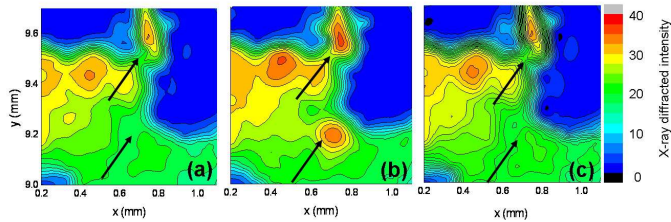


FIG. 4. Bragg peak intensity map of the $(1/4\ 1/4\ 0)$ reflection of the $\text{Pr}_{0.5}\text{Ca}_{0.5}\text{MnO}_3$ thin film at $T=50$ K. Before (a), and after (b) exposure to the x-rays in the two positions (indicated by the arrows) for approximately 60 minutes. All experiments are performed at 50 K with 643.25 eV with π incident polarization. X-ray exposure effects were erased by warming up the sample above T_{oo} as shown in the pattern collected after cooling (c).

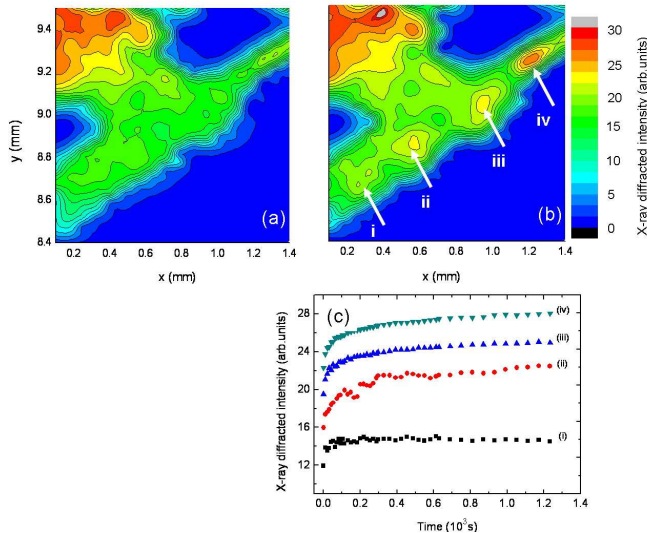


FIG. 5. Bragg peak intensity map of the $(1/4\ 1/4\ 0)$ reflection of the $\text{Pr}_{0.5}\text{Ca}_{0.5}\text{MnO}_3$ film at $T=50$ K before (a), and after (b) exposing with different x-ray conditions (see text) at four positions indicated by arrows, where in (c) the time dependence of the x-ray Bragg intensity at these positions is illustrated. The different curves are shifted to each other along the vertical axis for clarity. Writing the information in position (i), 3×10^{12} photons/s were used with as beam size of $100 \times 50\ \mu\text{m}$ [15]. Position (ii) was exposed to 6×10^{12} photons/s where for positions (iii) and (iv) we exposed with 1.2×10^{13} and 2.14×10^{13} photons/s, respectively. The vertical spot size varied from 50 (position (i) and (ii)), to 100 (position (iii)), and 200 μm for position (iv).

by creating defects in the magnetic and orbital ordered state, improving the long range order associated with the antiferromagnetic state. As a result the manganese magnetic moments re-align from a collinear antiferromagnetic structure to a canted structure with ferromagnetic components along the c-axis. As x-rays can be focused down to the sub micro-meter level it could

represent a new way for writing simultaneous magnetic and electronic information into a material. Moreover, the strength of changes can be varied by either tuning the x-ray flux density or by changing the exposure time. This novel effect is not only interesting in the understanding of the physics of strongly correlated systems, but it may also offer a novel route to manipulate magnetism.

The authors would like to acknowledge the beamline staff for the vital support as well as Dr. P.M. Derlet for improving the text style. This work has been supported by the Swiss National Science Foundation and National Centre of Competence in Research-Materials with Novel Electrical Properties and its the Japan Society for the Promotion of Science (JSPS) through the ‘‘Funding Program for World-Leading Innovative R&D on Science and Technology (FIRST Program)’’, initiated by the Council for Science and Technology Policy (CSTP). The work was carried out at the SIM beamline at the Swiss Light Source, Paul Scherrer Institut, Villigen, Switzerland.

* urs.staub@psi.ch

- [1] Y. Tokura, *Colossal Magnetoresistive Oxides* Ch.1 (Gordon & Breach Science Publishers, Amsterdam, 2000).
- [2] M. Rini, R. Tobey, N. Dean, J. Itatani, Y. Tomioka, Y. Tokura, R. W. Schoenlein & A. Cavalleri, *Nature* **449**, 72 (2007).
- [3] P. Beaud, S. L. Johnson, E. Vorobeva, U. Staub, R. A. De Souza, C. J. Milne, Q. X. Jia, and G. Ingold, *Phys. Rev. Lett.* **103**, 155702 (2009).
- [4] N. Takubo, Y. Ogimoto, M. Nakamura, H. Tamaru, M. Izumi and K. Miyano, *Phys. Rev. Lett.* **95**, 017404 (2005).
- [5] V. Kiryukhin, D. Casa, J. P. Hill, B. Keimer, A. Vigliante, Y. Tomioka & Y. Tokura, *Nature* **386**, 813 (1997).
- [6] Y. Horibe, C. H. Chen, S.-W. Cheong and S. Mori, *Europhys. Lett.* **70**, (3) 383-389 (2005).
- [7] E. F. Garman and R. L. Owen, *Acta. Cryst. D* **62**, 32-47 (2006).
- [8] J.B. Goodenough, *Phys. Rev.* **79**, 564 (1955).
- [9] Z. Jirak, S. Krupička, Z. Šimša, M. Dlouhá & S. Vratislav, *J. Magn. Magn. Mater.* **53**, 153 (1985).
- [10] H. Wadati, J. Geck, E. Schierle, R. Sutarto, F. He, D. G. Hawthorn, M. Nakamura, M. Kawasaki, Y. Tokura and G. A. Sawatzky, arXiv:1111.4725v1.
- [11] K. J. Thomas, J. P. Hill, S. Grenier, Y.-J. Kim, P. Abbamonte, L. Venema, A. Rusydi, Y. Tomioka, Y. Tokura, D. F. McMorrow, G. Sawatzky and M. van Veenendaal, *et al*, *Phys. Rev. Lett.* **92**, 237204 (2004).
- [12] U. Staub, M. García-Fernández, Y. Bodenthin, V. Scagnoli, R. A. De Souza, M. Garganourakis, E. Pomjakushina and K. Conder, *Phys. Rev. B* **79**, 224419 (2009).
- [13] S. Y. Zhou, Y. Zhu, M. C. Langner, Y.-D. Chuang, P. Yu, W. L. Yang, A. G. Cruz Gonzalez, N. Tahir, M. Rini, Y.-H. Chu, R. Ramesh, D.-H. Lee, Y. Tomioka, Y. Tokura, Z. Hussain, and R. W. Schoenlein, *Phys. Rev. Lett.* **106**, 186404 (2011).

- [14] U. Staub, V. Scagnoli, Y. Bodenthin, M. García-Fernández, R. Wetter, A. M. Mulders, H. Grimmer and M. Horisberger, *J. Synchron. Rad* **15**, 469 (2008).
- [15] U. Fleschig, F. Nolting, A. Fraile Rodríguez, J. Krem-paský, C. Quitmann, T. Schmidt, S. Spielmann, and D. Zimoch, *AIP Conference Proceedings* **1234**, 319 (2010).
- [16] U. Staub, V. Scagnoli, A. M. Mulders, K. Katsumata, Z. Honda, H. Grimmer, M. Horisberger and J. M. Tonnerre, *Phys. Rev. B* **71**, 214421 (2005).
- [17] J. P. Hill and D. F. McMorrow, *Acta Crystallogr. Sect. A* **52**, 236 (1996).
- [18] D. V. Lang, *Deep centres in Semiconductors* (ed. Pantelides, S.T.) **489-539** (Gordon & Breach, New York, 1986).